Dielectric Changes in Membrane Properties and Cell Interiors of Human Mesothelial Cells *in Vitro* after Crocidolite Asbestos Exposure

Elke Dopp,[1,2] Ludwig Jonas,[3] Barbara Nebe,[4] Axel Budde,[4] and Eberhard Knippel[4]

[1]Department of Biology, Institute of Cell Physiology and Biosystems Technology, University of Rostock, Rostock, Germany; [2]Institute of Hygiene and Occupational Health, University of Essen, Essen, Germany; [3]Department of Pathology, [4]Department of Internal Medicine, University of Rostock, Germany

Asbestos induces cytogenetic and genotoxic effects in cultured cell lines *in vitro*. For further investigations of the fiber-induced cellular changes, electrorotation (ROT) measurements can be used to determine early changes of surface properties and dielectric cellular changes. In the present study, human mesothelial cells (HMC) were exposed to nontoxic concentrations of crocidolite asbestos (1 µg/cm^2) for 12, 24, 30, 50, and 72 hr, and were investigated for changes in dielectric properties, morphologic and biochemical changes using ROT measurements, electron microscopy, and flow cytometry, respectively. The results of ROT measurements revealed slightly increased internal conductivity and decreased membrane conductance of HMC during the first 12 hr of exposure to crocidolite. This may be due to functional changes of ion channels of the cellular membrane. However, after exposures of ≥ 30 hr, reduced internal conductivity and increased membrane conductance of HMC occurred. These effects may be caused by permeabilization of the cell membrane and the leakage of ions into the surrounding medium. The membrane capacitance of HMC is always decreased during exposure of cells to crocidolite fibers. This decreased membrane capacitance may result from the observed reduction in the number of microvilli and from the shrinkage of cells as observed by electron microscopy and flow cytometry. Changes in composition of the plasma membrane were also observed after the labeling of phosphatidylserines (PS) on the cell surface. These observed changes can be related to apoptotic events. Whereas during the first 50 hr of exposure only a small number of HMC with increased exposure of PS on the cell surface was detected by flow cytometry, the dielectric properties of HMC showed marked changes during this time. Our results show that surface property changes of the cellular membrane of HMC as well as interior dielectric changes occur after the exposure of cells to crocidolite fibers. The observed changes are discussed in terms of complex combined cellular effects after amphibole asbestos exposure. *Key words*: apoptosis, crocidolite, electron microscopy, electrorotation, flow cytometry, phosphatidylserine, plasma membrane. *Environ Health Perspect* 108:153–158 (2000). [Online 10 January 2000]
http://ehpnet1.niehs.nih.gov/docs/2000/108p153-158dopp/abstract.html

The epidemiologic associations between asbestos exposure and malignant lung diseases (pleural mesothelioma, bronchogenic carcinoma) and fibrotic diseases (pleural plaques and asbestosis) are well known (*1*). However, the mechanisms linking the exposure of humans to asbestos and the subsequent development of these diseases are largely unknown. Various types of asbestos have been assessed for their genotoxic properties, using karyotypic and morphologic approaches in a number of rodent and human cell lines (*2*). These studies revealed differences in responses to asbestos in various cell types. Mesothelial cells are the target cells of asbestos-induced mesothelioma. Asbestos induces genotoxic changes and apoptosis in human mesothelial cells [(HMC); (*3,4*)], but until now early changes of surface properties as well as cellular dielectric parameters were not investigated after the exposure of cells to asbestos *in vitro*. Such investigations can supply more information about morphology and permeability of the cellular membrane and about dielectric parameters of the cytoplasm reflecting ion concentration, polarization of membranes of cytoplasmic compartments (organelles), dielectric relaxation of biomolecules (protein, DNA, amino acid, and small polypeptides), and ionic or protonic displacement along protein structures associated with the cytoskeleton.

Such information can be obtained from electrorotation (ROT) measurements characterizing electrical and dielectrical properties of cells. The ROT of cells is a useful technique for studying the dielectric properties of individual cells under conditions of minimal physiologic damage (*5*). The investigation of the effects of chemicals and environmental factors on the dielectric behavior of cells is increasingly becoming an area of scientific interest. ROT was used to characterize alterations of dielectric properties of lymphocytes (*6*), cell membrane changes after viral infection and transformation (*7–9*) as well as platelet activation (*10*), biofilms (*11*) and microbial contamination (*12*), the effect of chemicals on cells (*13*), cytoplasmatic dielectric properties (*14*), different cellular compartments of individual cells (*15*), and mobile charges on membranes (*16*). Rotation at physiologic ionic strength (*17*) and low-frequency ROT of erythrocytes (*18*) have also been studied. All of these ROT studies were performed using conventional microscopes for rotation measurements. Cell rotation in these studies was measured by "eye and stopwatch." In our laboratories, we developed a computerized automated instrumentation that makes ROT measurements more objective, productive, and comfortable (*19*) as compared to the conventional techniques. The new instrumentation allows objective measurements with a considerable productivity (~ 10 cells within one measuring cycle of 10 sec).

The phospholipid content can be measured to analyze changed morphology of the cellular membrane. The two major classes of the plasma membrane (PM) phospholipids, the choline- and aminophospholipids, are distributed asymmetrically between the two leaflets of the PM. Sphingomyelin and phosphatidylcholine make up the majority of the outer leaflet, whereas ethanolamine and serine phospholipids reside predominantly in the leaflet facing the cytosol (*20*). Recently it was found that so-called flippases (translocases) flip phosphatidylserines (PS) from the cytoplasm-facing leaflet to the opposite orientation (*21*) if apoptotic cellular changes occur (*22*). Such changes in PM structure can also influence dielectric properties of the cell.

Goodglick et al. (*23*) studied the membrane-damaging effect of asbestos and suggested that asbestos-induced lipid peroxidation may be part of the damaging mechanisms resulting in apoptosis. Early and late stages of apoptosis can be discriminated depending on the PS content of the plasma membrane. Annexin V is a calcium-dependent

Address correspondence to E. Dopp, Universität Essen, Universitätsklinikum, Institut für Hygiene und Arbeitsmedizin, Hufelandstraße 55, 45147 Essen, Germany. Telephone: 49 0201 723 4578. Fax: 49 0201 723 4546. E-mail: elke.dopp@uni-essen.de

We thank J. Saedler, B. Gnich, and I. Poser for excellent technical assistance; P. Emmerich, M. Barten, J. Zendeh, and T. Heller for obtaining ascites fluid; and Q. Rahman, D.G. Weiss, and D. Schiffmann for critical reading of the manuscript. We also thank E. Schwarz and G. Fulda for preparation and support in analysis of the electron microscopic samples, respectively.

This work was supported by DFG (Deutsche Forschungsgemeinschaft) grant no. Kn. 385/1-2, the Medical Faculty of the University of Rostock (FORUN-Programme 1997), and the Kultusministerium of Mecklenburg/Vorpommern (HSP III).

Received 1 June 1999; accepted 2 September 1999.

phospholipid-binding protein that preferentially binds to PS but shows minimal binding to other phospholipid species on the external surface (*24*). During the early stage of apoptosis, PS translocase is inhibited and the increased exposure of PS to the external surface of the cell potentially provides a signal to surrounding phagocytes (*25*).

In the current study, we investigated the time course of changes of the plasma membrane and cell interior after the exposure of HMC to crocidolite asbestos. We were interested in determining when surface properties of amphibole asbestos-treated cells begin to change, what kind of changes occur, and which relationship exists to the dielectric parameters of the cytoplasm. For these investigations, dielectric properties of the cell membrane and the cytoplasm were analyzed by ROT measurements and the translocation of PS to the external surface was measured in dependence on exposure time (12–72 hr) using flow cytometry. Electron microscopy was used to study the possible relationship between membrane capacitance as assessed by ROT measurements and cell surface structure.

Material and Methods

Cell culture and treatment conditions. We obtained HMC by effusion of ascites fluid from noncancerous patients at the University Hospital in Rostock, Germany. Fluid samples were centrifuged and the pelleted cells were transferred to 25-cm^2 tissue culture flasks (Nunc, Wiesbaden, Germany) and grown in a 1:1 mixture (v/v) of M199 and MCDB 105 medium (Sigma, Deisenhofen, Germany) supplemented with 5–10 ng/mL epidermal growth factor, 0.4 µg/mL hydrocortisone, and 7% fetal calf serum. The isolated mesothelial cells were identified and characterized by their positive staining for cytokeratins, using a panepithelial monoclonal antibody against human cytokeratins AE1/AE3 (Biofenex, San Ramon, CA). After the fourth passage, HMC changed into giant genomically instable cells with an irregular pattern and a lack of intracellular cytokeratin expression. Because of this phenomenon only HMC of the first passage were used for the experiments. Mesothelial cells were treated with a nontoxic concentration of crocidolite asbestos [Union Internationale Contre le Cancer (UICC) standard; 1 µg/cm^2]. The average fiber length, diameter, and number of fibers per microgram were determined. The average dimensions for chrysotile and crocidolite were 0.10 and 0.25 µm in diameter and 2.24 and 1.71 µm in length, respectively. The percentage of asbestos fibers with length ≥ 5 µm was approximately 5% for both types of asbestos fibers. Fibers were sterilized by autoclaving (120°C for 20 min) and were suspended in PBS.

ROT measurements. The general driving force of the particle rotation is a phase difference between the electric field-induced polarization and the external rotating field. This gives rise to a torque acting on the particle that depends on the frequency of the applied field, the geometry, and dielectic properties of the particle (*18,26–28*). ROT is a sensitive, noninvasive method for studying the dielectric properties of individual viable cells under conditions of minimal physiologic damage. There is general agreement that the dielectric characteristics of cells are closely associated with their biologic function and constitute a physical component of the cell phenotype (*10,18,27–33*).

We used automated instrumentation for ROT measurements, as described previously (*19*). Briefly, the device consists of a microscope with a rotation chamber, a video camera, and a computer that includes a field generator. Four rectangular signals in phase quadratur are applied to platinum–iridium electrodes to provide a rotating electric field. The cell rotation induced by this field is measured as a function of the field frequency ranging from 1 Hz to 24 MHz. The software developed for automated measurements allowed us to perform the entire operation including video digitalization, object recognition, tracking, calculation of the rotation speed of single objects, selection of objects, storage, and representation as well as statistic analysis of the data.

For ROT measurements, we washed untreated and fiber-treated HMCs twice in sodium chloride solution (conductivity 24 µS/cm) containing glucose to achieve the osmolarity of 300 mOsm. One hundred microliters of this suspension was sealed into the rotation chamber and measured immediately after the settling of the cells. Every point of the rotation curve represented measurements of 20–30 cells. The ROT spectrum consisted of 15 measuring points and was usually completed within 20–30 min. Cell rotation induced by the applied rotating field was measured as a function of the field frequency ranging from 1.5 kHz to 24 MHz. The measured data were fitted to a function containing two Lorentz functions. Heights and center points of the Lorentz functions were calculated to achieve a minimum deviation to the measured rotation velocity. The Lorentz functions corresponded to the first-order approximation of the theoretical curves, which were too complex for straight fitting of the cell parameters.

The reproducibility of the automated rotation measurement was performed by measuring the same cell population repeatedly (*19*). The mean variability over the whole frequency range was approximately 4%.

From the ROT spectrum four dielectric parameters can be derived: specific membrane capacity and conductivity (which reflect membrane thickness, composition, morphologic complexity, and the transport of charge carriers across the membrane) and cell internal conductivity and permittivity (reflecting the electrical mobility of ion species and the combined properties of cytoplasmic water and intracellular barriers to charge movement, respectively). These dielectric properties are derived qualitatively from changes of magnitude and frequency of the antifield and co-field peaks as compared to theoretical curves (*18,27,28,34*).

Electron microscopy. For transmission electron microscopy (TEM), treated and untreated cells were fixed with 4% glutaraldehyde in 0.1-M phosphate buffer for 1 hr, washed in the same buffer, and postfixed with 1% OsO_4. The samples were dehydrated, embedded, polymerized, and sectioned in the usual manner. After the preparation of ultrathin sections with an Ultrotom III (LKB, Sweden) and contrasting with uranyl acetate and lead citrate, the samples were examined in an EM 902A transmission electron microscope (Zeiss, Jena, Germany).

For scanning electron microscopy (SEM), the adherent cell cultures were fixed with 4% glutaraldehyde in PBS for 1 hr, washed, postfixed with 1% OsO_4, dehydrated with alcohol, and critical point dried. The cells were examined in the adherent stage after coating with gold in a DSM 960A scanning electron microscope (Zeiss).

Flow cytometry. Annexin-V-fluorescein isothiocyanate (FITC) (PharMingen Deutschland GmbH, Hamburg, Germany) was used to quantitatively determine the percentage of HMC with an increased level of exposed PS on the cell surface. These changes can be related to apoptotic events. The assay is based on the fact that PS is exposed on the surface of irreversibly damaged cells, and the assay makes use of the high affinity of annexin-V for PS. Treated and untreated mesothelial cells were washed with cold PBS, centrifuged, and resuspended in 1 × binding buffer (10 mM Hepes/NaOH, 140 mM NaCl, 2.5 mM $CaCl_2$). Approximately 10^5 cells were incubated with 0.25 µg/mL FITC-conjugated annexin-V and 5 µg/mL propidium iodide (PI). After staining, the cells were measured within 45 min.

We analyzed the cells with a FACSort flow cytometer (Becton Dickinson, Heidelberg, Germany) with data acquisition. We performed data analysis using CELLQuest Software (Becton Dickinson). Ten thousand cells per sample were measured.

Results

The ROT spectrum of untreated cells is shown in Figure 1. Various mammalian cells typically have two rotation peaks: antifield rotation at frequencies below 3 MHz (due to

the presence of a nonconducting plasma membrane) and co-field rotation above 3 MHz (as a result of the difference in the dielectric properties of the surrounding medium and the cell interior) (*7*). The curves presented in Figures 1 and 2 were fitted to get minimal deviation from measured data. The maximal rotation velocity for untreated HMC was found at 15 kHz. After a 12-hr treatment with crocidolite, the antifield peak moved to a frequency of 40 kHz and the rotation speed increased approximately four times (Figure 1). The mean relative deviation between the two curves in Figure 1 was 38%. The magnitude of the antifield rotation was increased and the peak occurred at a higher frequency. Furthermore, magnitude and frequency of the co-field rotation were also changed, although to a smaller extent (Figure 1).

After 30 hr of fiber treatment, the peak shifted to a frequency of 200 kHz (Figure 2). The rotation speed of the treated cells decreased up to 75% as compared to that found in untreated cells.

In contrast to the early phase shown in Figure 1, this later phase was characterized by a decreased magnitude and an increased frequency of the antifield rotation. A decreased membrane capacity was also observed. After 50 hr of exposure to crocidolite, the antifield peak shifted toward the control population. After an exposure time of 72 hr, the difference to the control measurements was only 15%.

Alterations of ROT spectra after crocidolite exposure, as shown in Figures 1 and 2, are significant corresponding to the variability of the rotation measurements. We measured the same cell population repeatedly to evaluate the variability of the automated rotation measurement. The measurements were compared using the following equations for mean rotation and SD:

$$\langle \omega \rangle = \sum_{i=1}^{n} \frac{\left|\omega_i^I\right| + \left|\omega_i^{II}\right|}{2}$$

$$SD = \sum_{i=1}^{n} \sqrt{\frac{\left(\omega_i^I - \omega_i^{II}\right)^2}{n \cdot (n-1)}}$$

where SD = standard deviation for all frequencies; w = rotation speed; and f = frequency. The variability SD/<ω> was 4%.

To determine if the observed effects of crocidolite-treated mesothelial cells were typical for this kind of cells, we treated another cell type, Syrian hamster embryo fibroblasts (SHE cells), with crocidolite asbestos under the same conditions. In the later phase after fiber treatment (> 30 hr), there was a significant difference in the dielectric behavior as compared to HMC (Figure 3). Whereas the frequency of the antifield peak increased for HMC, SHE cells were characterized by a corresponding decrease of frequency. The peak height was decreased in both cases.

SEM as well as TEM studies revealed a changed cell surface of HMC after treatment with crocidolite (Figure 4). Long slender microvilli can be observed in the untreated control cells (Figure 4 A, B). After 12 hr the number of microvilli was already decreased (Figure 4 C, D) and after 48 hr an extensive loss of microvilli was detected in crocidolite-exposed HMC (Figure 4 E, F). Furthermore, cytotoxic effects were detectable after the exposure of cells to crocidolite asbestos. After an exposure time of > 48 hr, cell shrinkage (Figure 5 A, C) and bleb formation were observed after the treatment of HMC with crocidolite asbestos. For quantification of cells with a reduced cell size, we performed light scatter measurements. Figure 5 B, D clearly show that the asbestos-treated cell population had a reduced cell size (forward scatter) and an increased granularity (side scatter). Measurements of cell size of 30 untreated control cells and 30 crocidolite-treated HMC using computer software (CorelDraw 8.0; Corel Corporation, Wien, Austria) revealed a reduction in size (control, 311.6 + 81.6 µm^2; crocidolite-treated HMC, 228.2 ± 133.6 µm^2; ≅ 73%) and extent (control, 122.2 ± 32.4 µm; crocidolite-treated HMC, 69.3 ± 29.7 µm; ≅ 56.5%).

TEM study of HMC showed a strong phagocytotic uptake of crocidolite fibers by uncoated invaginations of the plasma membrane and the accumulation of fibers inside lysosomes and residual bodies. Membrane accumulations such as myelin structures at the end of fibers inside residual bodies are typical after the uptake of crocidolite fibers. Effects after the exposure of cells to chrysotile (UICC standard) were similar but weaker (data not shown). Typical features of apoptotic cells, such as dehydration of cytoplasm, vesiculation, and bleb formation on the cell surface, fragmentation of nuclei, and chromatin separation, were also observed by TEM in asbestos-exposed HMC (> 70 hr).

A PS plasma membrane asymmetry was detected by flow cytometry in amphibole asbestos-exposed HMC after labeling PS with Annexin V. Within 50 hr after exposure to crocidolite asbestos, annexin V-binding to HMC was measured at a minor extent (16–18%). In the untreated control up to 12% of the cells showed Annexin-V binding [mean, 8.7% ± 2.7%; (Figure 6)]. An increase (up to 40%) of annexin V-binding to PS can be observed only after 70 hr of exposure to crocidolite (Figure 6). Interestingly, our results after the exposure of HMC to chrysotile (1 µg/cm^2) were completely different: The chrysotile data (Figure 6) are shown for comparison. Even after 30 hr of exposure to chrysotile, the number of cells detected by annexin V is significantly higher as compared to the crocidolite-treated cells (Figure 6).

Mesothelial cells exposed to cisplatin (50 µM) for 24 hr were used as the positive control. We detected 58.6 + 10.3% of cells with exposed PS on the surface in the positive control.

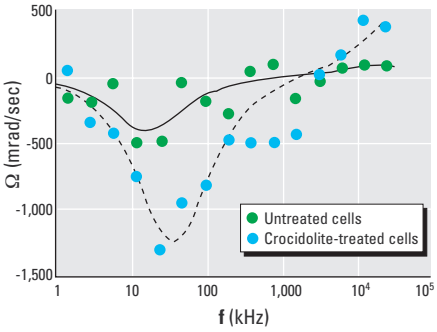

Figure 1. ROT spectra (rotation velocity vs. frequency of the rotating field) of untreated (solid line) and crocidolite-treated (dotted line) HMC (concentration, 1 µg/cm^2; exposure time, 12 hr). Each point of the rotational curves of untreated and crocidolite-treated cells represents the mean of 20–30 cells.

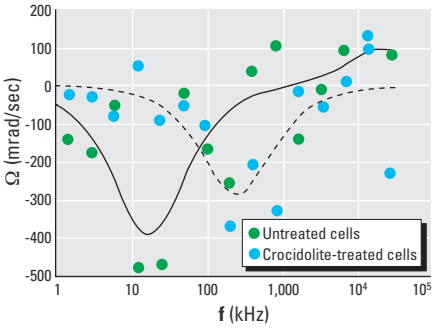

Figure 2. ROT spectra of untreated (solid line) and crocidolite-treated (dotted line) HMC (concentration, 1 µg/cm^2; exposure time, 30 hr). Each point of the rotational curves of untreated and crocidolite-treated cells represents the mean of 20–30 cells.

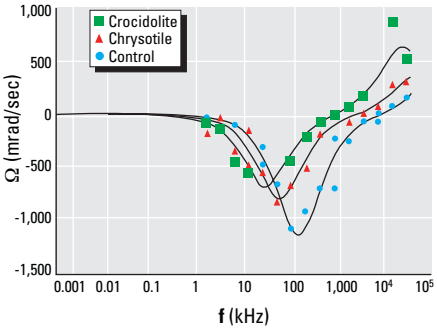

Figure 3. ROT spectra of untreated, crocidolite-treated, or chrysotile-treated Syrian hamster embryo fibroblasts (control population: concentration, 1 µg/cm^2; exposure time, 30 hr). Each point of the rotational curves of untreated, crocidolite-treated, and chrysotile-treated cells represents the mean of 20–30 cells.

Discussion

Conventional dielectrophoresis and ROT measurements have revealed that significant differences exist in the dielectric properties of cells in different physiologic states (*14,35–37*). These findings demonstrate that cell dielectric characteristics are closely associated with biologic function and collectively constitute a physical component of cell phenotype. This dielectric phenotype provides a new additional criterion for the classification of cells.

Asbestos has several effects in cultured cells, including mesothelial cells, such as induction of gene expression (*38*), production of growth factors and cytokines (*39*), inhibition of growth (*40*), induction of damage to chromosomes (*41*) and DNA (*40*), transformation (*42*), and apoptosis (*43*). To date, almost nothing is known about early surface property changes of the cellular membrane and interior dielectric changes of asbestos-treated cells. In the present study we found that two different phases of ROT spectra existed after the treatment of HMC with crocidolite asbestos. The first phase was detectable after 12 hr and lasted approximately 18 hr. In this early phase after fiber treatment, crocidolite induced an impairment of the membrane charge carrier transposition system followed by an increased interior conductivity and decreased membrane conductivity. In the second phase (> 30 hr exposure), a decreased internal conductivity and an increased membrane conductivity occurred, which can be interpreted as a result of permeabilization of the plasma membrane and leakage of ions into the surrounding medium.

According to the theory of Georgieva et al. (*27*), the behavior of the antifield peak in the early phase of the ROT spectra can be interpreted as a result of injury to the plasma membrane charge carrier transposition system (membrane channels, pores, and pumps). This is characterized by a decreased membrane conductance and by increased internal conductivity. Therefore, it is important to consider that the apparent membrane conductivity is composed of a tangential and transverse surface conductance component. However, according to minor changes in the surface charge of cells (and therefore surface conductance), we can assume that alterations of membrane conductivity are mainly represented by the transverse component and thus can be interpreted as a changed transport of charge carriers across the membrane. Changes of magnitude and frequency of the co-field rotation peak confirmed this interpretation of increased interior conductivity. At the same time the internal permittivity decreased; this may be due to increasing viscosity and/or the decreasing mobility of water molecules. According to changes of the antifield and co-field peak, the membrane capacitance was reduced during the first hours after crocidolite exposure. It seems reasonable to interpret this result in a manner similar to those obtained for the later phase, where we also found a reduction of the membrane capacitance. A decrease in the morphologic complexity and/or cell shrinking can be expected to change the membrane dielectric properties before these processes are visible by electron microscopy.

The ROT behavior of HMC 30 hr after treatment with crocidolite was considerably changed as compared to the early phase and can be interpreted as permeabilization of the cellular membrane and its increased conductivity (which reflects the transposition of charge carriers across the membrane). At the same time, the internal conductivity of the cells decreased due to the leakage of ions into the surrounding medium. However, the plasma membrane generally appears to be so well preserved that the cell contents are sealed within the cells.

The cell membrane consists of a lipid bilayer into which proteins and other biomolecules are incorporated. Lipid bilayer capacity is mainly determined by the nonpolar

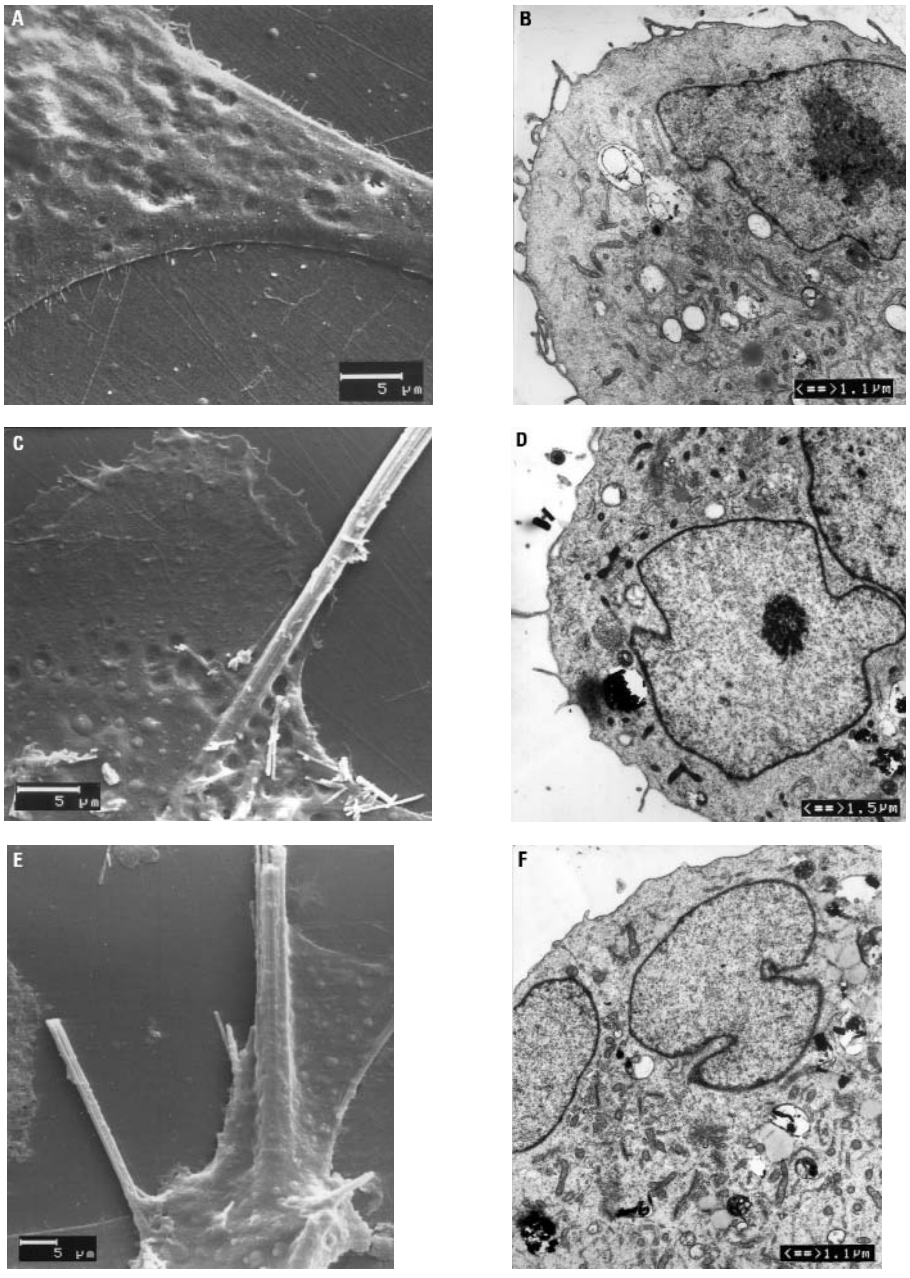

Figure 4. Scanning and transmission electron microscopy of HMC. (*A*) and (*B*) show untreated cells from SEM and TEM, respectively. Microvilli are detectable on the cell surface. (*C*) and (*D*) show SEM and TEM results, respectively, after the treatment of HMC with crocidolite asbestos (1 µg/cm^2); the loss of microvilli can be observed after an exposure time of only 12 hr. (*E*) and (*F*) show that after a 48-hr exposure, microvilli are no longer detectable by SEM and TEM, respectively.

hydrocarbon groups and the number of carbon atoms in the lipid hydrocarbon chain (*44*), whereas the contribution of integral proteins to the dielectric properties of the cell membrane is dominated by the nonpolar amino acid residues (*45*). The actual total area of membrane covering a cell is larger than we can assume for a smooth surface. This is due to surface features such as microvilli, folds, and blebs. We found a marked reduction in microvilli. However, microvilli that may represent a potential reservoir of membrane material to facilitate cell division and rapid changes in morphology (*46*) increase the cell surface area. Reduced membrane capacitance may be the consequence of a decreased number of microvilli. However, the continuous shrinking of cells, as observed in the later phase, can also cause a decreased membrane capacitance if the reduced surface area and the possible delivery of membrane-bound water are taken into account. In addition, the membrane capacitance can also be influenced by changes in membrane-molecule polarization that can appear after PS translocation. The observed decrease of membrane capacitance is probably a complex process that originates from more than one event.

After 50 and 72 hr of exposure to crocidolite, we found the same, albeit clearly reduced, effect on HMC. This reduction can be explained by the incubation procedure. The cell cultures were grown after exposure to fibers, which led to an increased portion of "normal" cells in the later phase.

According to the ROT theory (*27*), the effect of crocidolite asbestos on SHE cells (control cells) can be interpreted as an increased membrane permeabilization characterized by an increased membrane conductivity and a decreased internal conductivity. This behavior, which has also been found in HMC, seems to be a more general effect of crocidolite independent of the kind of used cells. The opposite effect of crocidolite on the antifield peak frequency of SHE cells as compared to HMC can be explained as an increased membrane capacitance, which is characteristic for increased morphologic complexity. This interpretation is confirmed by the increased peak height and the decreased frequency of the co-field peak after crocidolite treatment. Altogether, the decreased morphologic complexity observed for HMC treated with crocidolite asbestos seems to be a more typical membrane reaction of this cell type. These results are comparable with earlier findings from Kodama et al. (*47*) and Dopp and Schiffmann (*48*). These authors reported differences in genotoxic effects between human and rodent cell lines.

An increased appearance of PS at the outer leaflet can influence the dielectric properties of cells, but it may also be related to apoptotic events (*49*). Several authors reported on the induction of apoptosis in mesothelial cells by asbestos fibers (*43,50–52*). Broaddus et al. (*43*) found that 6% of rabbit pleural mesothelial cells (RPMC) showed an increased annexin-V fluorescence intensity (6%) in flow cytometry analysis after only 2 hr of exposure to crocidolite (concentration, 3 μg/cm^2; control level, 2%). After a 6-hr exposure, 10% of early apoptotic cells were measured (control, 3%), and after a 24-hr exposure, 21% of RPMC were apoptotic. Longer exposure times were not investigated.

In the present experiments, only annexin V- and propidium iodide-labeling were carried out. Detection of apoptotic cells requires more biologic end points.

Our results of flow cytometry show that the number of crocidolite-treated HMC with an increased level of PS on the cell surface increases rapidly after a longer exposure time (> 50 hr), but early changes already start after a few hours of exposure. The number of cells with exposed PS at the outer leaflet is relatively high in the untreated control (8–12%). This is possible because we used adherent cell cultures for our investigations and we had to trypsinize the cultures for flow cytometry studies. Van Engeland et al. (*53*) described specific membrane-damaging effects during the harvesting of cells, thus allowing annexin-V-FITC to bind to internally located PS. This can result in a small percentage of false-positive results (~ 5%). Nevertheless, all of the cell cultures were treated in the same way.

The time course of PS exposure (and possibly of the induction of apoptosis) in HMC is different after the treatment of cells with crocidolite or chrysotile. In previous investigations we showed that chrysotile induces apoptosis to a much higher extent (*54*), but we did not monitor the time course. One possible reason for the different time courses of induction of PS exposure

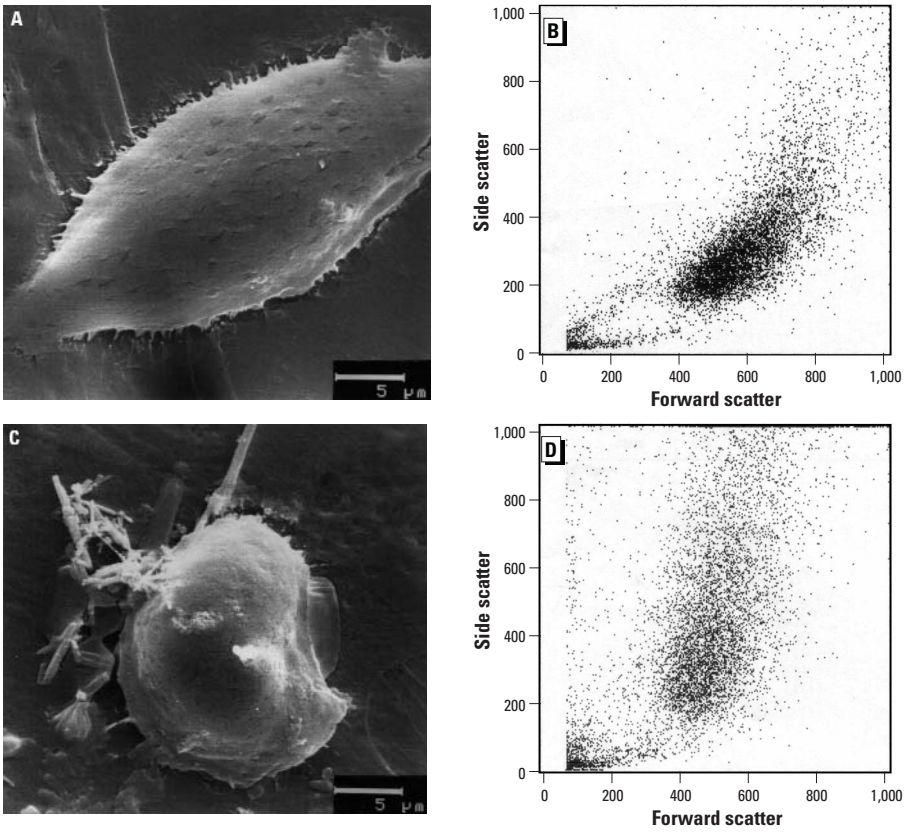

Figure 5. SEM and flow cytometry measurements of untreated (*A*) and (*B*), respectively, crocidolite treated (*C*) and (*D*), respectively, HMC. After an exposure time of 30 hr (fiber concentration, 1 μg/cm^2), cell shrinkage can be observed (*C*), and flow cytometry results clearly show a reduced cell size (forward scatter) and an increased granularity (side scatter).

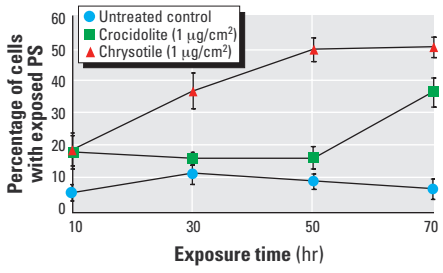

Figure 6. Detection of HMC with exposed PS on the cell surface. HMC were incubated with annexin V (PS binding) and propidium iodide (DNA stain) and measurements were carried out by flow cytometry. Chrysotile data are shown for comparison.

may be the different chemical composition of crocidolite and chrysotile (amphibole and serpentine asbestos, respectively). Chrysotile is hollow and its iron content is low, in contrast to crocidolite. Crocidolite is a more carcinogenic fiber, and chrysotile induces higher numbers of micronucleated and apoptotic cells (*54,55*). The induction of cellular changes and finally of apoptosis seem to be different and seem to depend on the type of fiber and, possibly, its physical properties.

In conclusion, changes of the dielectric properties of the plasma membrane and the cell interior after the treatment of HMC with crocidolite fibers can be determined from the ROT spectra. The effect of crocidolite fibers on the dielectric behavior of HMC is already detectable after a short exposure time (12 hr). In connection with the changed dielectric properties of HMC, we found an extensive loss of microvilli, a reduced cell size, an increased granularity, and an increased PS exposure at the outer leaflet of the plasma membrane. It is possible that the observed early cellular changes caused by amphibole asbestos fibers are affiliated components of the initiation step of the multistage process of carcinogenesis. Further mutational events are necessary (promotion step). Each of the successive events is likely to make the cell more unstable so that the risk of subsequent changes or apoptotic cell death increases.

Reference and Notes

1. Mossman BT, Gee JBL. Asbestos-related diseases. N Engl J Med 320:721–730 (1989).
2. Mossman BT. Carcinogenesis and related cell and tissue response to asbestos: a review. Ann Occup Hyg 38:617–624 (1994).
3. BeruBe KA, Quinlan TR, Fung H, Magae J, Vacek P, Taatjes DJ, Mossman BT. Apoptosis is observed in mesothelial cells after exposure to crocidolite asbestos. Am J Respir Cell Mol Biol 15:141–147 (1996).
4. Goldberg JL, Zanella CL, Janssen YM, Timblin CR, Jimenez LA, Vacek P, Taatjes DJ, Mossman BT. Novel cell imaging techniques show induction of apoptosis and proliferation in mesothelial cells by asbestos. Am J Respir Cell Mol Biol 17: 265–271 (1997).
5. Fuhr G, Zimmermann U, Shirley SG. Electromanipulation of Cells. Boca Raton, FL:CRC Press, Inc., 1996.
6. Xun H, Arnold WM, Zimmermann U. Alterations in the electrical properties of T and B lymphocyte membranes induced by mitogenic stimulation. Activation monitored by electrorotation of single cells. Biochim Biophys Acta 1021:191–200 (1990).
7. Wang XB, Huang Y, Gascoyne PRC, Becker FF, Hölzel R, Pethig R. Changes in Friend murine erythroleukaemia cell membranes during induced differentiation determined by electrorotation. Biochim Biophys Acta 1193:330–344 (1994).
8. Gascoyne PRC, Pethig R, Satayavivad J, Becker FF, Ruchirawat M. Dielectrophoretic detection of changes in erythrocyte membranes following malarial infection. Biochim Biophys Acta 1323:240–252 (1997).
9. Huang Y, Wang XB, Becker FF, Gascoyne PRC. Membrane changes associated with the temperature-sensitive P85 (gag-mos)-dependent transformation of rat kidney cells as determined by dielectrophoresis and electrorotation. Biochim Biophys Acta 1282:76–84 (1996).
10. Gimsa J, Pritzen C, Donath E. Characterization of virus-red-cell interaction by electrorotation. Biophys J 130:123–131 (1989).
11. Xiao-Feng Z, Markx GH, Pethig R, Eastwood IM. Differentiation of viable and non-viable bacterial biofilms using electrorotation. Biochim Biophys Acta 1245:85–93 (1995).
12. Burt JPH, Chan KL, Daeson D, Parton A, Pethig R. Assays for microbial contamination and DNA analysis based on electrorotation. Ann Biol Clin 54:253–257 (1996).
13. Zhou XF, Markx GH, Pethig R. Effect of biocide concentration on electrorotation spectra of yeast cells. Biochim Biophys Acta 1281:60–64 (1996).
14. Huang Y, Wang XB, Hölzel R, Becker FF, Gascoyne PRC. Electrorotational studies of the cytoplasmic dielectric properties of Friend murine erythroleucaemia cells. Phys Med Biol 40:1789–1806 (1995).
15. Hölzel R, Lamprecht I. Dielectric properties of yeast cells as determined by electrorotation. Biochim Biophys Acta 1104:195–200 (1992).
16. Sukhorukov VL, Zimmermann U. Electrorotation of erythrocytes treated with dipicrylamine: mobile charges within the membrane show their "signature" in rotational spectra. J Membr Biol 153:161–169 (1996).
17. Gimsa J, Schnelle T, Fuhr G. Dielectric spectroscopy of single human erythrocytes at physiological ion strength: dispersion of the cytoplasm. Biophys J 71:495–506 (1996).
18. Sauer FA, Schlögel RW. Torques exerted on cylinders and spheres by external electromagnetic fields: a contribution to the theory of field induced electrorotation. In: Interactions between Electromagnetic Fields and Cells (Chiabrera A, Nicolini C, Schwan HP, eds). New York: Plenum Press, 1985;123–134.
19. Budde A, Grümmer G, Knippel E. Electrorotation of cells and particles-an automated instrumentation. Instr Sci Technol 27:59– 66 (1999).
20. Devaux PF. Static and dynamic lipid asymmetry in cell membranes. Biochemistry 30:1163–1173 (1991).
21. Tang XJ, Halleck MS, Schlegel RA, Williamson P. A subfamily of P-type ATPases with aminophospholipid transporting activity. Science 272:1495–1597 (1996).
22. Van den Eijnde SM, Boshart L, Reutelingsperger CPM, De Zeeuw C, Vermeij-Keers C. Phosphatidylserine plasma membrane asymmetry in vivo: a pancellular phenomenon which alters during apoptosis. Cell Death Differ 4:311–316 (1997).
23. Goodglick LA, Pietras LA, Kane AB. Evaluation of the causal relationship between crocidolite asbestos-induced lipid peroxidation and toxicity to macrophages. Am Rev Respir Dis 139:1265–1273 (1989).
24. Andree HA, Reutelingsperger CP, Hauptmann R, Hemker HC, Hermens WT, Willems GM. Binding of vascular anticoagulant alpha (VAC alpha) to planar phospholipid bilayers. J Biol Chem 265:4923–4928 (1990).
25. Walton M, Sirimanne E, Reutelingsperger C, Williams C, Gluckman P, Dragunow M. Annexin V labels apoptotic neurons following hypoxia-ischemia. Neuroreport 8:3871–3875 (1997).
26. Arnold WM, Zimmermann U. Electrorotation: development of a technique for dielectric measurements on individual cells and particles. J Electrostat 21:151–191 (1988).
27. Georgieva R, Neu B, Shilov VM, Knippel E, Budde A, Latza R, Donath E, Kiesewetter H, Bäumler H. Low frequency electrorotation of fixed red blood. Biophys J 74:2114–2120 (1998).
28. Wang XB, Huang Y, Hölzel R, Burt JPH, Pethig R. Theoretical and experimental investigations of the interdependence of the dielectric, dielectrophoretic and electrorotational behaviour of colloidal particles. J Phys D Appl 26:312–322 (1993).
29. Arnold WM, Geier BM, Wendt B, Zimmermann U. The change in the electrorotation of yeast cells effected by silver ions. Biochim Biophys Acta 889:35–48 (1986).
30. Fuhr G, Geißler F, Müller T, Hagedorn R, Torner H. Differences in the rotation spectra of mouse oocytes and zygotes. Biochim Biophys Acta 930:65–71 (1987).
31. Fuhr G, Rösch P, Müller T, Dressler V, Göring H. Dielectric spectroscopy of chloroplasts isolated from higher plants: characterization of the double-membrane system. Plant Cell Physiol 31:975–985 (1990).
32. Donath E, Egger M, Pastuschenko V. Dielectric behaviour of the anion-exchange protein of human red blood cells. Theoretical analysis and comparison to electrorotation data. Bioelectrochem Bioenerg 23:337–360 (1990).
33. Sukhorukov VL, Arnold WM, Zimmermann U. Hypotonically induced changes in the plasma membrane of cultured mammalian cells. J Membr Biol 132:27–40 (1993).
34. Eppmann P, Gimsa J, Prueger B, Donath E. Dynamic light scattering from oriented, rotating particles: a theoretical study and comparison to electrorotation data. J Phys (Paris) 6:421–432 (1996).
35. Egger M, Donath E. Electrorotation measurements of diamide-induced platelet activation changes. Biophys J 68:364–372 (1995).
36. Irimajiri A, Hanai T, Inouye T. A dielectric theory of "multistratified shell" model with its application to a lymphoma cell. J Theor Biol 78:251–269 (1979).
37. Marszalek P, Zielinski JJ, Fikus M, Tsong TY. Determination of electric parameters of cell membranes by a dielectrophoresis method. Biophys J 59:982–987 (1991).
38. Heintz NH, Janssen YM, Mossman BT. Persistent induction of c-*fos* and c-*jun* expression by asbestos. Proc Natl Acad Sci USA 90:3299–3303 (1993).
39. Boylan AM, Rüegg C, Kim KJ, Hebert CA, Hoeffel JM, Pytela R, Sheppard D, Goldstein IM, Broaddus VCJ. Evidence of a role for mesothelial cells-derived interleukin-8 in the pathogenesis of asbestos-induced pleurisy in rabbits. Clin Invest 89:1257–1267 (1992).
40. Dong H, Buard A, Renier A, Levy F, Saint-Etienne L, Jaurand MC. Role of oxygen derivatives in the cytotoxicity and DNA damage produced by asbestos on rat pleural mesothelial cells in vitro. Carcinogenesis 15:1251–1255 (1994).
41. Lechner JF, Tokiwa T, LaVeck M, Benedict WF, Bands-Schlegel S, Yeager H, Banerjee A, Harris CC. Asbestos-associated chromosomal changes in human mesothelial cells. Proc Natl Acad Sci USA 82:3884–3888 (1985).
42. Hesterberg TW, Barrett JC. Dependence of asbestos- and mineral dust-induced transformation of mammalian cells in culture on fiber dimensions. Cancer Res 44:2170–2180 (1984).
43. Broaddus VC, Yang L, Scavo LM, Ernst JD, Boylan AM. Asbestos induces apoptosis of human and rabbit pleural mesothelial cells via reactive oxygen species. J Clin Invest 98:2050–2059 (1996).
44. Risbo J, Jorgensen K, Sperotto MM, Mouritsen OG. Phase behaviour and permeability properties of phospholipid bilayers containing a short-chain phospholipid permeability enhancer. Biochim Biophys Acta 1329:85–96 (1997).
45. Pethig R, ed. Dielectric and Electronic Properties of Biological Materials. Chichester:Wiley, 1979.
46. Mutsaers SE, Whitaker D, Papadimitriou JM. Changes in the concentration of microvilli on the free surface of healing mesothelium are associated with alterations in surface membrane charge. J Pathol 180:333–339 (1996).
47. Kodama Y, Boreiko CJ, Maness SC, Hesterberg TW. Cytotoxic and cytogenetic effects of asbestos on human bronchial epithelial cells in culture. Carcinogenesis 14:691–697 (1993).
48. Dopp E, Schiffmann D. Analysis of chromosomal alterations induced by asbestos and ceramic fibers. Toxicology Lett 96/97:155–162 (1998).
49. Fadok VA, Voelker DR, Campbell PA, Cohen JJ, Bratton DL, Henson PM. Exposure of phosphatidylserine on the surface of apoptotic lymphocytes triggers specific recognition and removal by macrophages. J Immunol 148:2207–2216 (1992).
50. Timblin CR, Guthrie GD, Janssen YW, Walsh ES, Vacek P, Mossman BT. Patterns of c-*fos* and c-*jun* proto-oncogene expression, apoptosis, and proliferation in rat pleural mesothelial cells exposed to erionite or asbestos fibers. Toxicol Appl Pharmacol 151:88–97 (1998).
51. Levresse V, Renier A, Fleury-Feith J, Levy F, Moritz S, Vivo C, Pilatte Y, Jaurand MC. Analysis of cell cycle disruptions in cultures of rat pleural mesothelial cells exposed to asbestos fibers. Am J Respir Cell Biol 17:660–671 (1997).
52. Jimenez LA, Zanella C, Fung H, Janssen YM, Vacek P, Charland C, Goldberg J, Mossman BT. Role of extracellular signal-regulated protein kinases in apoptosis by asbestos and H_2O_2. Am J Physiol 273:1029–1035 (1997).
53. Van Engeland M, Ramaekers FCS, Schutte B, Reutelingsperger CPM. A novel assay to measure loss of plasma membrane asymmetry during apoptosis of adherent cells in culture. Cytometry 24:131–139 (1996).
54. Dopp E, Nebe B, Hahnel C, Papp T, Alonso B, Simko M, Schiffmann D. Mineral fibers induce apoptosis in Syrian hamster embryo fibroblasts. Pathobiology 63:213–221 (1995).
55. Dopp E, Schuler M, Schiffmann D, Eastmond DA. Induction of micronuclei, hyperdiploidy and chromosomal breakage affecting the centric/pericentric regions of chromosomes 1 and 9 in human amniotic fluid cells after treatment with asbestos and ceramic fibers. Mutat Res 377:77–87 (1997).